CCTV lenses for video meteor astronomy

Mariusz Wiśniewski [1], *Arkadiusz Olech* [2], *Mirosław Krasnowski* [3], *Kamil Złoczewski* [4],
Krzysztof Mularczyk [5], *Piotr Kędzierski* [6], *and Wojciech Jonderko* [7]

We present the results of CCTV lens tests made last year at the Ostrowik Observatory by observers of the Comets and Meteors Workshop. A total of 13 lenses with different parameters were tested. The limiting magnitudes, size of field of view, distortion and off-axis aberrations were measured. The Computar $f/1.2$, $f = 4$ mm appeared to be the best lens tested. We also note the good marks of both Ernitecs which were finally chosen as the lenses which will be used in our projects. Surprisingly, the very fast lenses which are popular in video meteor astronomy seem to be much worse that their $f/1.2$ rivals.

1 Introduction

One of the key indispensable elements for video observations of meteors is a good lens. The quality of the resulting image of the sky depends not only on the detector characteristics but also on the lens quality. A poor lens can produce images with large off-axis optical aberrations, distortion and vignetting, causing problems with determining the properties of meteors observed at the edge of the field.

Lenses for CCTV (closed-circuit television) are cheap but quite complicated devices. Typically, their optics contain many lense elements made with different kinds of glass, with different shapes in different structures and arrangements. It is not easy to build a good quality instrument at that small size. Thus the lenses of different manufacturers with the same parameters could produce completely different results.

During the last two years, the Polish *Comets and Meteors Workshop (CMW)* started two projects which use video techniques extensively. These are the *Polish Automated Video Observations (PAVO)* project (Wiśniewski et al. 2003) and the *Polish Fireball Network* (Olech et al., in preparation). These projects are financially supported by Siemens Building Technologies and Factor Security. Of course the funds are limited and thus we are interested in buying only equipment with the best quality to price ratio. Thanks to Factor Security we had access to many CCTV lenses offered by this company and thus we decided to test their usefulness in meteor astronomy.

2 Parameters and properties

Optical parameters of CCTV lenses are described in the same way as for photographic lenses: f/x, where x is

some number, tells us how fast a lens is[1] and $f = x$ is its focal length (for example $f/1.2$, $f = 8$ mm). The ratio of these gives us the diameter of a lens which is the most important factor in determining the amount of light gathered by our equipment.

There is relection and refraction of light at each air-to-glass surface. Of course we want to avoid reflection. The reflected light does not hit our detector, causes a decrease of the lens' optical efficiency and produces ghost images. In a typical air-to-glass surface about 95% of light goes through it but 5% is reflected. This looks as a small number, but typical lens contains more than 10 such surfaces. This gives us a transmission of $0.95^{10} \sim 0.60$ and as much as 40% of the light lost!

To solve this problem, manufacturers of optical instruments cover the lenses with thin layers of materials such as MgF_2, SiO_2 or TiO_2. The most sophisticated multilayer coatings made by top manufacturers can decrease the light loss at one air-to-glass surface even down to 0.2%.

3 Fighting the aberrations

Light going through lenses can suffer from the influence of many aberrations. We list them here briefly. For further details of these, see textbooks on optics such as (Hecht, 1998; Ray, 1977; Welford, 1991).

Chromatic aberration is the result of dispersion in the glass and occurs when shorter wavelength light is refracted more than longer wavelength. In other words a lens that suffers from chromatic aberration will have a different focal length for each color. In color CCTV cameras this produces violet rings around bright stars.

In most common cases, the surface of a single lens is a section of a sphere since this is the easiest shape to make. But with a spherical surface, incoming rays from different distances from the optical axis focus at slightly different points along the axis. So if the center of the image stays in focus and is bright, the edges of the field appear blurry and dimmer. This effect is called spherical aberration.

Coma (Latin, related to the origin of the word 'comet') is off-axis spherical aberration caused by rays entering the lens at an angle. Due to this phenomenon,

[1] Nicolaus Copernicus Astronomical Center, Bartycka 18, 00-716 Warsaw, Poland. Email: `mwisniew@camk.edu.pl`

[2] Nicolaus Copernicus Astronomical Center, Bartycka 18, 00-716 Warsaw, Poland. Email: `olech@camk.edu.pl`

[3] ul. Zjazd 6, Poznań, Poland. Email: `mirek@post.pl`

[4] Warsaw University Astronomical Observatory, Al. Ujazdowskie 4, 00-478 Warsaw, Poland. Email: `kzlocz@astrouw.edu.pl`

[5] Warsaw University Astronomical Observatory, Al. Ujazdowskie 4, 00-478 Warsaw, Poland. Email: `kmularcz@astrouw.edu.pl`

[6] Warsaw University Astronomical Observatory, Al. Ujazdowskie 4, 00-478 Warsaw, Poland.

[7] ul. Pod Walem 23, 44-203 Rybnik, Poland. Email: `wjonderko@go2.pl`

[1] This strange but traditional notation describes the focal ratio f/d, where f is the focal length and d the lens diameter. For example '$f/1.2$, $f = 8$ mm' says that the diameter is $f/1.2$, i.e. 8/1.2 or 6.7 mm. *–Editor.*

Figure 1 – The 13 lenses tested.

point-like images of stars become blurry comet-like structures at the edge of the field of view.

Astigmatism is another off-axis aberration. The incoming rays passing through the lens at oblique angles with respect to the optical axis focus differently from paraxial rays. (See the *Glossary* below.) Depending on the incidence angle of the off-axis rays entering the lens, the refracted plane is oriented either tangentially or sagittally. So the resulting image depends upon the location in the focal plane and thus produces blurry images, more or less elongated, of which the intensity and contrast decrease as the distance from the center increases.

Distortion is an effect of the focal length of the lens varying with the distance from the optical axis. As a result some parts of the image are more magnified than others. Distortion occurs in two main forms: barrel and pincushion, also called negative and positive distortion respectively.

Figure 2 – The experimental setup for the tests.

Glossary

Optical axis: the axis through the centre of all the lens elements, at right-angles to them.

Paraxial: a light ray not parallel to the optical axis, but at only a small angle to it.

Chief ray: a ray passing through the centre of a lens element, but at an angle to the optical axis.

Tangential: consider a plane which contains both the optical axis and the chief ray: this is the tangential plane. A ray within this plane, but not passing though the centre of the lens element, is a tangential ray.

Meridional (plane or ray): synonym for tangential (plane or ray).

Sagittal: consider a plane which contains the chief ray but is at right-angles to the tangential plane: this is the sagittal plane. A ray within this plane, but not passing though the centre of the lens element, is a sagittal ray.

Table 1 – Basic parameters of the tested lenses. (a): auto iris (adjusts automatically to light level); (z): zoom. F: focal ratio, i.e. f/d. FWHM: stellar image width. Columns dist$_1$ and dist$_2$ are measured in percentages of the distance from the image center to the corner. For an explanation of other quantities, see the Section 4.

Name	f (mm)	F	FOV (°)	FWHM (pix)	LM_s (mag)	LM_l (mag)	OE %	dist$_{max}$ (pix)	dist$_1$ (%)	dist$_2$ (%)
ERNITEC (a)	2.8	1.4	120.8	1.82	0.70	6.26	49	-2.608	85	100
COMPUTAR	8.0	1.2	43.2	1.89	3.98	8.51	54	-2.654	78	100
SIEMENS	12.0	1.2	27.9	1.86	4.30	8.88	33	0.697	100	100
COMPUTAR	4.0	1.2	91.2	1.69	2.95	7.76	94	17.976	57	62
ERNITEC	8.0	1.2	42.1	1.52	3.65	8.55	47	-4.106	62	73
SIEMENS	4.0	1.2	85.6	1.84	2.30	6.88	47	12.536	66	76
PENTAX	8.0	1.2	42.1	2.18	3.41	8.57	43	1.998	92	100
SIEMENS	6.0	1.2	55.9	1.93	3.86	7.90	72	-7.934	62	69
TAMRON (z)	2.8	1.4	103.4	1.86	1.34	6.14	59	-18.150	53	59
EVETAR	12.0	1.4	29.7	2.25	3.65	8.50	28	-0.940	100	100
TAMRON (z)	3.0	1.0	115.2	2.00	1.84	6.43	38	-4.927	62	71
SIEMENS (a)	4.0	1.2	85.6	2.18	2.91	6.57	61	12.254	57	67
COMPUTAR (a)	3.8	0.8	90.9	2.72	2.06	5.74	14	4.946	64	74

The CCTV detector is always a flat plane but the resulting image plane given by the lens is not. This phenomenon is called field curvature and produces problems with obtaining sharp images across the whole field of view.

4 Tests

Our tests were made on 2004 February 21 at the Ostrowik station of Warsaw University Astronomical Observatory. In total, we tested the 13 lenses shown in Figure 1; their basic parameters are given in Table 1.

As a detector we used a monochrome Mintron MTV-13V3 camera with a frame integration function available. The images from the camera were recorded with a high quality Panasonic AG-TL300 video recorder. First, we checked the appearance of the sky for single frame normal mode. Second, we used the integration mode of the Mintron camera. We recorded images made by accumulating 128 frames. For normal and integrated modes the exposure times were of 0.02 and 2.56 sec, respectively. Integrated mode gave us a chance to see more faint stars and to find even slight differences between the limiting magnitudes of particular lenses. All the optical defects described above are more visible in integrated images. Our testing equipment is shown in Figure 2.

We used a Matrox Meteor II card to convert analog images into digital form. We used the grab program, which is a part of MetRec package (Molau 1994, 1995, Molau & Nitschke 1996, Molau et. al 1997). Examples of integrated images are shown in Figures 3 and 4. We grabbed images at the resolution of 384 × 288 pixels used by MetRec software. (This software halves the horizontal and vertical resolution with 2×2 binning.)

4.1 Image deformation

We looked for distortion effects on long exposure images. We used the Refstars program (Molau, 1992) to identify stars. Observed stars' positions were compared with the theoretical positions for ideal optics. The graphs showing the differences (in pixels) between the observed and correct positions of the stars as a function of the distance of the star from the center of the FOV (field of view, also in pixels) are shown in Figure 5 (page 29). The field sizes (in percentages of the distance from the image center to the corner) at which the above-mentioned difference is below 1 pixel (dist$_1$) and 2 pixels (dist$_2$) are given in Table 1. This table shows also the maximal difference (dist$_{max}$) which was measured for each lens.

Distortion has an influence on the true field of view. Knowing the positions of the stars in our recorded images, we were able to determine true fields of view and compare them to those given by the manufacturers.

4.2 Limiting magnitude and optical efficiency

The determination of limiting magnitudes for long and short exposures was made by eye by three persons independently and the results averaged. Limiting magnitudes, after correcting to the same size of aperture, translate into the optical efficiency.

4.3 Star images

An ideal lens would produce almost point-like images of stars across the whole FOV of the camera. Of course this was not the case for lenses tested by us. Aberrations such as coma, astigmatism, field curvature and chromatic aberration combine to produce stellar images which are blurry and elongated. To estimate this effect we measured the profiles (FWHM[2]) of about 100 star images per recorded long exposure frame. The mean values of FWHM derived for each lens are also shown in Table 1.

----

[2]Full width, half maximum. This describes the full width (i.e. edge to edge, not center to edge) at which the intensity has fallen to half the maximum.
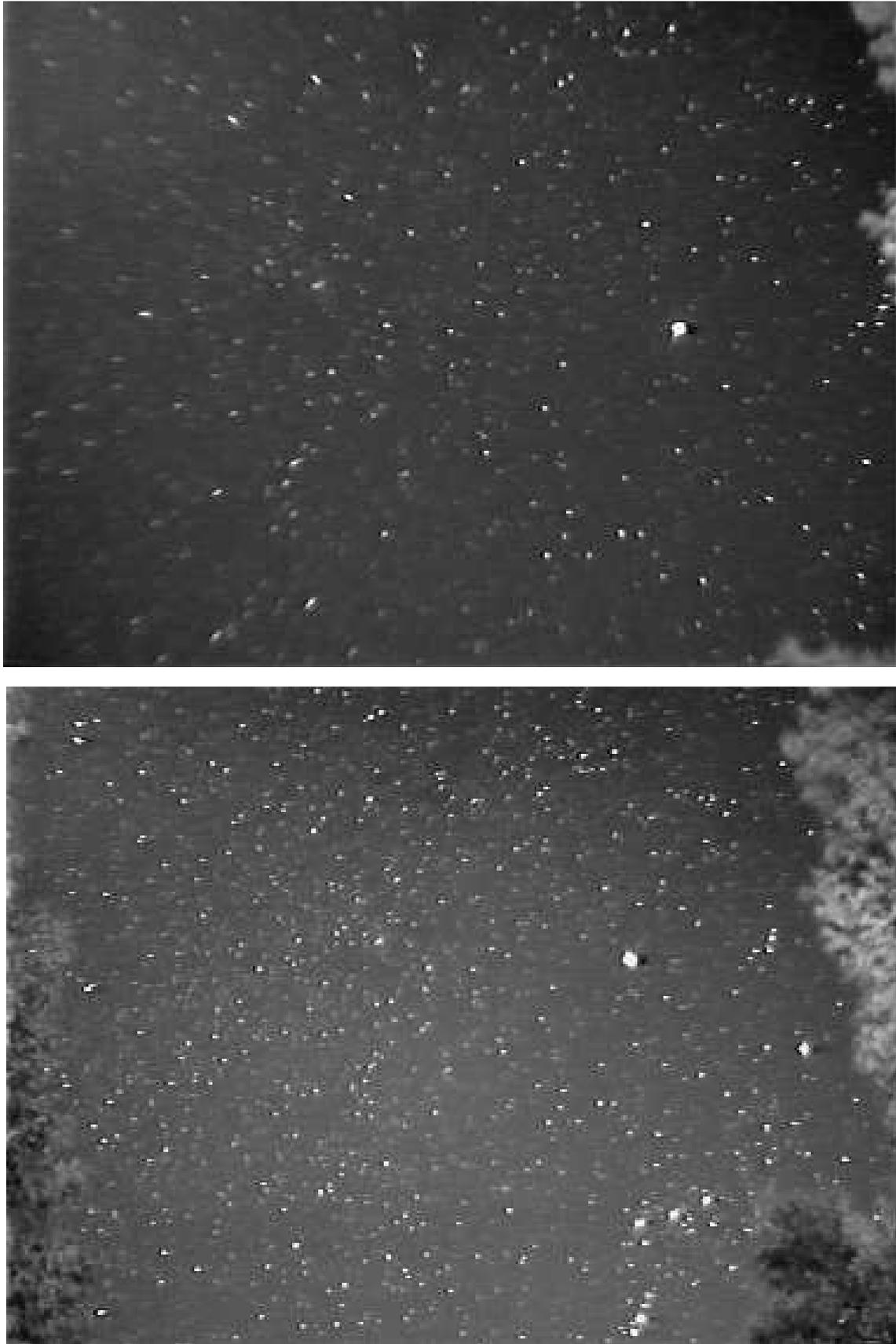
Figure 3 – Example of images for long exposures. Top: EVETAR $f/1.4$, $f = 12$ mm. The cheapest and the worst picture quality lens. Bottom: ERNITEC $f/1.2$, $f = 8$ mm. The most focused image. These images have been enlarged so that the pixels are visible, to allow a critical appraisal of the quality.

Figure 4 – Example of images for long exposures. Top: COMPUTAR $f/1.2$, $f = 4$ mm. The best lens in the tests. Bottom: COMPUTAR $f/0.8$, $f = 3.8$ mm. The fastest lens in the tests. These images have been enlarged so that the pixels are visible, to allow a critical appraisal of the quality.

Table 2 – Final results of the test, with results measured in points rather than physical units. (a): auto iris (adjusts automatically to light level); (z): zoom. F: focal ratio, i.e. f/d. FWHM: stellar image width. For an explanation of other quantities, see the Section 4.

Name	f (mm)	F	FWHM (0–10)	OE (0–10)	$\mathrm{dist_{max}}$ (0–3)	$\mathrm{dist_1}$ (0–3)	$\mathrm{dist_2}$ (0–6)	Total (0–32)
ERNITEC (a)	2.8	1.4	9	6	2.1	2.4	6.0	25.5
COMPUTAR	8.0	1.2	8	6	2.1	2.1	6.0	24.2
SIEMENS	12.0	1.2	8	4	2.7	3.0	6.0	23.7
COMPUTAR	4.0	1.2	10	10	0.3	0.9	2.4	23.6
ERNITEC	8.0	1.2	10	6	1.5	1.2	4.2	22.9
SIEMENS	4.0	1.2	9	6	0.3	1.8	4.8	21.9
PENTAX	8.0	1.2	5	5	2.4	2.7	6.0	21.1
SIEMENS	6.0	1.2	7	8	0.9	1.2	3.6	20.7
TAMRON (z)	2.8	1.4	8	7	0.3	0.6	1.8	17.7
EVETAR	12.0	1.4	3	3	2.7	3.0	6.0	17.7
TAMRON (z)	3.0	1.0	7	4	1.2	1.2	3.6	17.0
SIEMENS (a)	4.0	1.2	5	7	0.6	0.9	3.0	16.5
COMPUTAR (a)	3.8	0.8	1	1	1.2	1.5	4.2	8.9

4.4 Criteria

A summary of our tests is given in Tables 1 and 2. The categories which were taken into account to get the final mark were: mean FWHM (0–10 points), OE - optical efficency, (0–10 points), $\mathrm{dist_{max}}$ - maximal distortion (0–3 points), $\mathrm{dist_1}$ - size of field of view with distortion below 1 pixel (0–3 points), $\mathrm{dist_2}$ - size of field of view with distortion below 2 pixels (0–6 points). An ideal lens would get the total number of 32 points. The numbers of points collected by each lens in each category and the total scores are presented in Table 2.

5 Conclusions

The best lenses in our tests were those produced by Ernitec and Computar. Our work was performed in order to choose the best lenses to use on video cameras of the *Polish Fireball Network*. We were mostly interested in 4 and 8 mm lenses and thus we have naturally chosen Computars and Ernitecs.

The results for very fast lenses were a big surprise for us. These two lenses had the worst optical efficiency and poor FWHM. They were also the most expensive among the lenses tested. We suppose that the materials used for their construction comes from the early 1990s. Thus their quality of, for example, multilayer anti-reflection coatings could be much worse than in those lenses currently manufactured.

Full results of our tests will be available on the *PFN* web page at `http://pfn.pkim.org` .

Acknowledgements

References

Hecht E. (1998). *Optics*. Addison-Wesley, Reading, Mass., USA, 3rd edition.

Molau S. (1994). "MOVIE: Meteor Observation with VIdeo Equipment". In Roggemans P., editor, *Proc. IMC, Puimichel, France*, pages 71–75. International Meteor Organization, Potsdam.

Molau S. (1995). "MOVIE — analysis of video meteors". In Knoefel, A. & Roggemans P., editor, *Proc. IMC, Belogradchik, Bulgaria*, pages 51–61. International Meteor Organization, Potsdam.

Molau S. and Nitschke M. (1996). "Computer-based meteor search: a new dimension in video meteor observation". *WGN*, **24:4**, 119–123.

Molau S., Nitschke M., de Lignie M., Hawkes R. L., and Rendtel J. (1997). "Video observations of meteors: history, current status, and future prospects". *WGN*, **25:1**, 15–20.

Olech A., Wiśniewski M., Żołądek P., Krasnowski M., Fietkiewicz K., Kwinta M., Dorosz D., Lemiecha A., Lemiecha M., Sajdak M., Turek P., Kędzierski P., Mularczyk K., Złoczewski K., Kowalski T., Kowalski Ł., Fajfer T., Wójcicki K., Szary A., and Kozłowski S. (2005). *WGN*. in preparation.

Ray S. (1977). *The Lens and All its Jobs*. Focal Press, London.

Welford W. (1991). *Useful Optics*. Univ. Chicargo Press, Chicargo.

Wiśniewski M., Kędzierski P., Mularczyk K., and Złoczewski K. (2003). "Polish Automated Video Observations (PAVO)". *WGN*, **31:1**, 33–34.
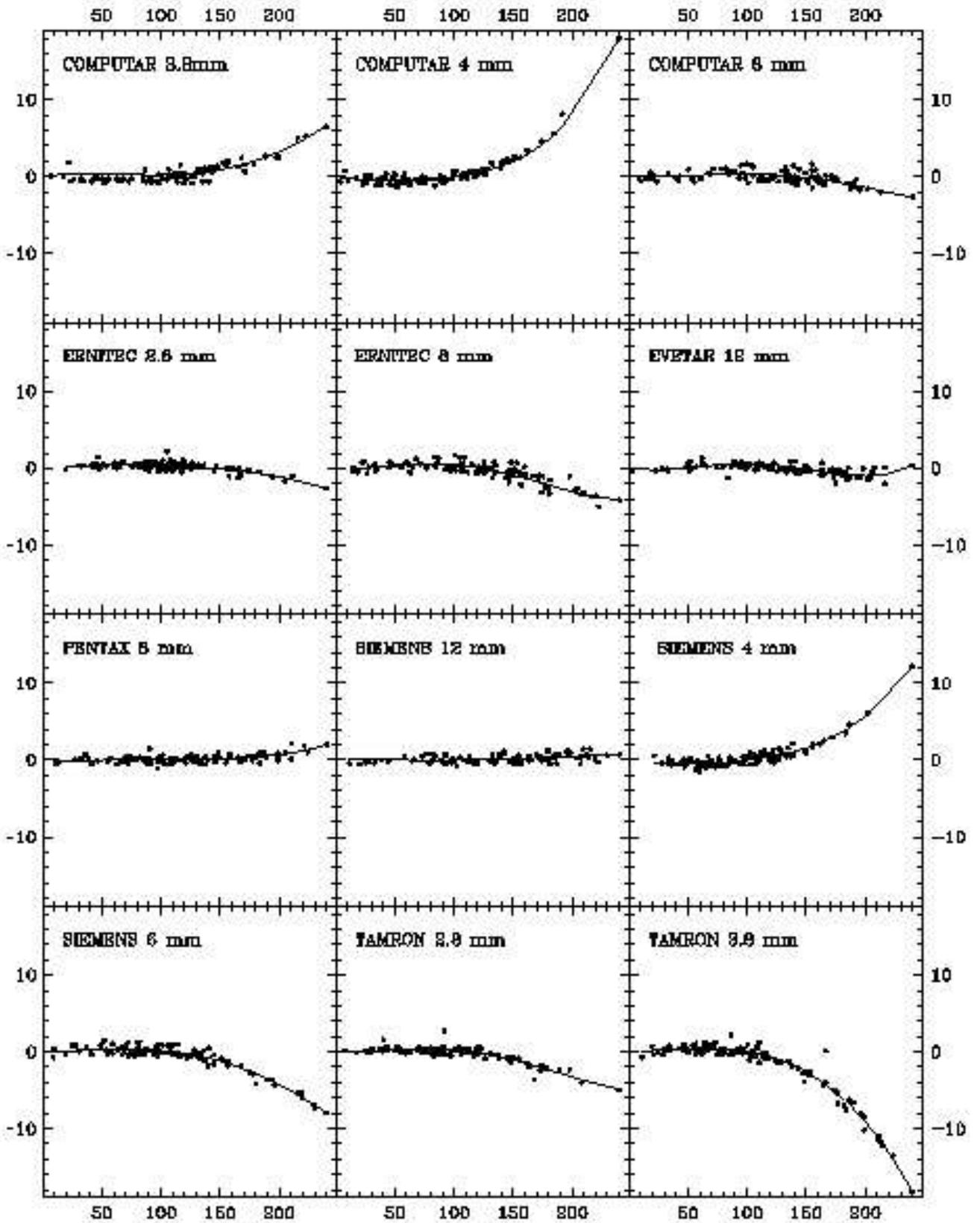
Figure 5 – Distortions of tested lenses as a function of distance from centre of view. Vertical axes: observed−correct positions, in pixels. Horizontal axes: distance from the center of the field of view, in pixels.